Novel Recognition of Thymine Base in Double-Stranded DNA by Zinc(II)−Macrocyclic Tetraamine Complexes Appended with Aromatic Groups

Emiko Kikuta, Mariko Murata, Naomi Katsube, Tohru Koike, and Eiichi Kimura*

Contribution from the Department of Medicinal Chemistry, Faculty of Medicine, Hiroshima University, Kasumi 1-2-3, Minami-ku, Hiroshima 734-8551, Japan

Received November 9, 1998

Abstract: DNase I footprinting has revealed that zinc(II) complexes with macrocyclic tetraamines (1,4,7,10-tetraazacyclododecane,cyclen) appended with one or two aryl-methyl group(s), ((9-acridinyl)methyl-, (4-quinolyl)methyl-, 1,7-bis(4-quinolyl)methyl-, (1-naphthyl)methyl-, and 1,7-bis(1-naphthyl)methyl-cyclen) selectively bind to native double-stranded DNA (150 base pairs), at AT-rich regions like classical minor groove binders (distamycin A and 4,6-diamidino-2-phenylindole (DAPI)). The selectivity and affinity depend on the stacking ability and number of the aromatic ring. Zn^{2+} is an essential metal ion for the DNA binding, which cannot be replaced by other metal ions such as Cu^{2+} or Ni^{2+}. The DNA binding by these Zn^{2+}−cyclen derivatives was inhibited by captopril having a stronger affinity for the fifth coordination site of the Zn^{2+}−cyclen complexes. Micrococcal nuclease footprinting, moreover, revealed that those Zn^{2+}−cyclen derivatives bound only to the thymine groups in the A−T base pairs, while distamycin A and DAPI simultaneously bound to the thymine and adenine groups in the A−T base pairs. Distamycin A and the Zn^{2+}−(4-quinolyl)methyl-cyclen reversibly competed for common AT-rich regions of minor groove. The DNA binding mode by the Zn^{2+}−cyclen derivatives was due to the selective and strong complex formation between the Zn^{2+}−cyclen moiety and the imide-deprotonated thymine at neutral pH.

Introduction

Small molecules recognizing specific DNA sequences have attracted great interest for gene-targeted drugs, which may alter the local structure of DNA to inhibit access of activators or repressors to regulate ultimate gene expression processes.[1] A number of clinically useful drugs such as distamycin A (**1**),[2] 4,6-diamidino-2-phenylindole (DAPI) (**2**),[2f−g,3] echinomycin (**3**),[4] actinomycin D,[2b−d,5] and cisplatin[6] interact with DNA in various fashions via hydrophobic, electrostatic, hydrogen-bonding, dipolar forces and/or coordinate interactions. Of these, distamycin A (**1**) and DAPI (**2**) are minor groove binders that recognize AT-rich regions. They simultaneously bind to adenine N(3) and thymine O(2) by hydrogen bondings and stabilize the A−T duplex structure (Scheme 1).[2,3] Currently, chemical modification of these minor groove binders has been actively undertaken.[7]

Scheme 1

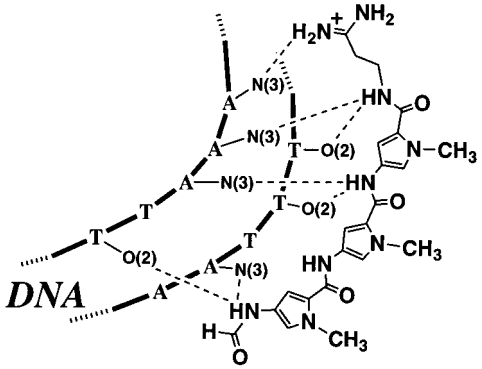

(1) (a) Zimmer, C.; Wähnert, U. *Prog. Biophys. Mol. Biol.* **1986**, *47*, 31−112. (b) Denison, C.; Kodadek, T. *Chem. Biol.* **1998**, *5*, R129−R145.

(2) (a) Coll, M.; Frederick, C. A.; Wang, A. H. J.; Rich, A. *Proc. Natl. Acad. Sci. U.S.A.* **1987**, *84*, 8385−8389. (b) van Dyke, M. W.; Hertzberg, R. P.; Dervan, P. B. *Proc. Natl. Acad. Sci. U.S.A.* **1982**, *79*, 5470−5474. (c) Fox, K. R.; Waring, M. J. *Nucleic Acids Res.* **1984**, *12*, 9271−9285. (d) van Dyke, M. W.; Dervan, P. B. *Nucleic Acids Res.* **1983**, *11*, 5555−5567. (e) Griffin, J. H.; Dervan, P. B. *J. Am. Chem. Soc.* **1987**, *109*, 6840−6842. (f) Woynarowski, J. M.; Sigmund, R. D.; Beerman, T. A. *Biochemistry* **1989**, *28*, 3850−3855. (g) Wilson, W. D.; Ratmeyer, L.; Zhao, M.; Strekowski, L.; Boykin, D. *Biochemistry* **1993**, *32*, 4098−4104. (h) Breslauer, K. J.; Remeta, D. P.; Chou, W.-Y.; Ferrante, R.; Curry, J.; Zaunczkowski, D.; Synder, J. G.; Marky, L. A. *Proc. Natl. Acad. Sci. U.S.A.* **1987**, *84*, 8922−8926.

(3) (a) Portugal, J.; Waring, M. J. *Biochim. Biophys. Acta* **1988**, *949*, 158−168. (b) Larsen, T. A.; Goodsell, D. S.; Cascio, D.; Grzeskowiak, K.; Dickerson, R. E. *J. Biomol. Struct. Dyn.* **1989**, *7*, 477−491. (c) Tanious, F. A.; Veal, J. M.; Buczak, H.; Ratmeyer, L. S.; Wilson, W. D. *Biochemistry* **1992**, *31*, 3103−3112. (d) Trotta, E.; D'Ambrosio, E.; Del Grosso, N.; Ravagnan, G.; Cirilli, M.; Paci, M. *J. Biol. Chem.* **1993**, *268*, 3944−3951. (e) Wilson, W. D.; Tanious, F. A.; Barton, H. J.; Jones, R. L.; Fox, K.; Wydra, R. L.; Strekowski, L. *Biochemistry* **1990**, *29*, 8452−8461.

(4) (a) van Dyke, M. W.; Dervan, P. B. *Science* **1984**, *225*, 1122−1127. (b) Low, C. M.; Drew, H. R.; Waring, M. J. *Nucleic Acids Res.* **1984**, *12*, 4865−4879. (c) Ughetto, G.; Wang, A. H.; Quigley, G. J.; van der Marel, G. A.; van Boom, J. H.; Rich, A. *Nucleic Acids Res.* **1985**, *13*, 2305−2323. (d) Bailly, C.; Hamy, F.; Waring, M. J. *Biochemistry* **1996**, *35*, 1150−1161.

(5) (a) Müller, W.; Crothers, D. M. *J. Mol. Biol.* **1968**, *35*, 251−290. (b) Sobell H. M.; Jain, S. C.; Sakore, T. D.; Nordman, C. E. *Nat. New Biol.* **1971**, *231*, 200−205. (c) Lane, M. J.; Dabrowiak, J. C.; Vournakis, J. N. *Proc. Natl. Acad. Sci. U.S.A.* **1983**, *80*, 3260−3264. (d) Chu, W.; Shinomiya, M.; Kamitori, K. Y.; Kamitori, S.; Carlson, R. G.; Weaver, R. F.; Takusagawa, F. *J. Am. Chem. Soc.* **1994**, *116*, 7971−7982.

(6) (a) Trimmer, E. E.; Zamble, D. B.; Lippard, S. J.; Essigmann, J. M. *Biochemistry* **1998**, *37*, 352−362. (b) Gelasco, A.; Lippard, S. J. *Biochemistry* **1998**, *37*, 9230−9239. (c) Takahara, P. M.; Rosenzweig, A. C.; Frederick, C. A.; Lippard, S. J. *Nature* **1995**, *377*, 649−652. (d) van Boom, S. S.; Yang, D.; Reedijk, J.; van der Marel, G. A.; Wang, A. H. *J. Biomol. Struct. Dyn.* **1996**, *13*, 989−998. (e) Yang, D.; van Boom, S. S.; Reedijk, J.; van Boom, J. H.; Wang, A. H. *Biochemistry* **1995**, *34*, 12912−12920. (f) Kline, T. P.; Marzilli, L. G.; Live, D.; Zon, G. *Biochem. Pharmacol.* **1990**, *40*, 97−113.

10.1021/ja983884j CCC: $18.00
Published on Web 05/29/1999

Scheme 2

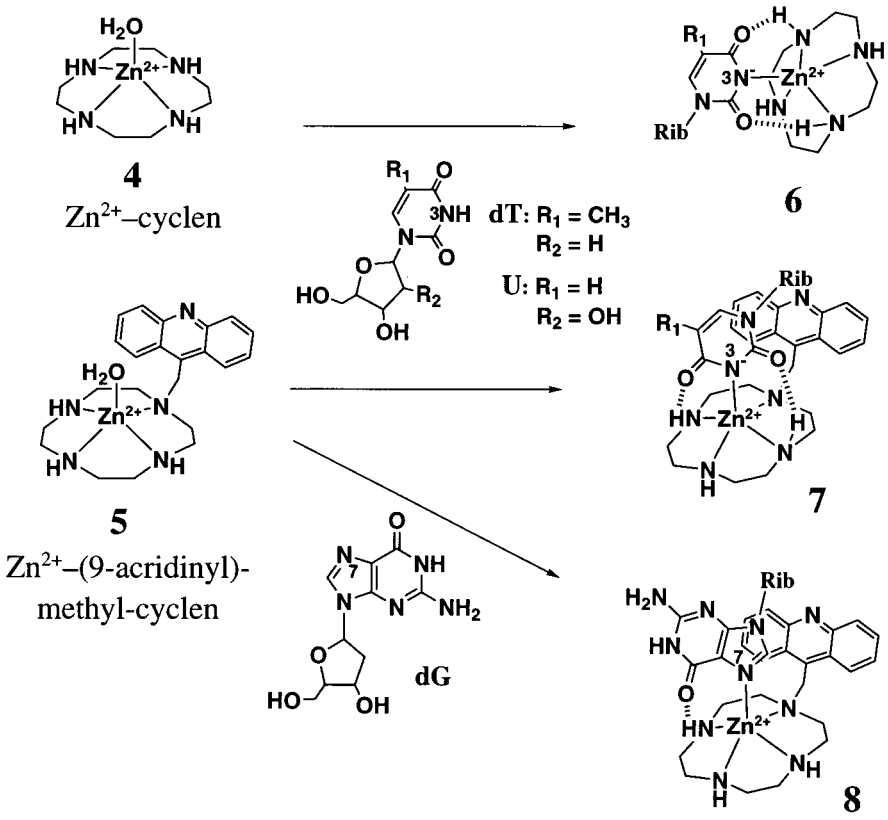

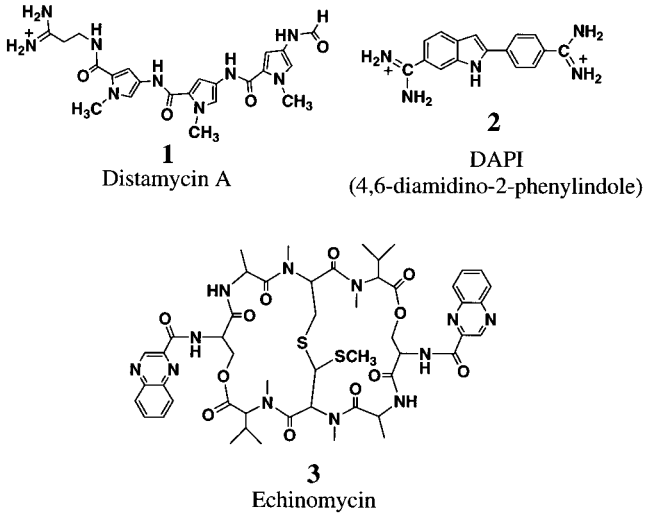

Recently, some macrocyclic tetraamine zinc(II) complexes, Zn^{2+}−cyclen **4** (cyclen = 1,4,7,10-tetraazacyclododecane),[8] Zn^{2+}−(9-acridinyl)methyl-cyclen **5**[9] and other Zn^{2+}−cyclen derivatives[10−15] were found to selectively bind to deoxythymidine (dT) and uridine (U) in aqueous solution at physiological pH (Scheme 2). In the resulting ternary complexes **6** and **7**, the nucleobases take N(3)-deprotonated anionic form (dT^- or U^-) to bind with Zn^{2+}. In addition, **5** showed an appreciably strong association with neutral deoxyguanosine (dG) to form **8** through a Zn^{2+}−N(7)(guanine) coordination, a hydrogen bond between the cyclen NH and O(6)(guanine), and a hydrophobic interaction between the two aromatic rings. Moreover, these Zn^{2+}−cyclen derivatives interact with dT^- and U^- in single-stranded poly(dT) and poly(U) with little interference from the anionic phosphate backbone.[12] In the interaction with U^- in double-stranded poly(A)·poly(U), **4** and **5** competed against adenine (A) so as to disrupt the natural A−U hydrogen bonds, melting the duplex of poly(A)·poly(U), as evidenced by physicochemical techniques such as the lowered T_m values and CD spectral change. Further, **5** appeared to interact with guanine base in double-stranded poly(dG)·poly(dC), probably from major groove to stabilize the double-stranded structure, as indicated by the higher T_m.

To find a more detailed interaction picture on DNA, we now have adopted a biochemical approach. With the use of appropriate DNA and the well-established DNA nuclease footprinting analysis technique,[16−18]one could easily obtain useful information of the sequence-selective properties of the Zn^{2+}−cyclen derivatives, as conducted for distamycin A (**1**)[2,17] and DAPI

(7) (a) Bailly, C.; Chaires, J. B.; *Bioconjugate Chem.* **1998**, *9*, 513−538. (b) Trauger, K. W.; Baird, E. E.; Dervan, P. B. *Nature* **1996**, *382*, 559−561. (c) Gottesfeld, J. M.; Neely, L.; Trauger, J. W.; Baird, E. E.; Dervan, P. B. *Nature* **1997**, *387*, 202−205. (d) Kielkopf, C. L.; White, S.; Szewczyk, J. W.; Turner, J. M.; Baird, E. E.; Dervan, P. B.; Rees, D. C. *Science* **1998**, *282*, 111−115 and references therein.

(8) Shionoya, M.; Kimura, E.; Shiro, M. *J. Am. Chem. Soc.* **1993**, *115*, 6730−6737.

(9) Shionoya, M.; Ikeda, T.; Kimura, E.; Shiro, M. *J. Am. Chem. Soc.* **1994**, *116*, 3848−3859.

(10) Tucker, J. H. R.; Shionoya, M.; Koike, T.; Kimura, E. *Bull. Chem. Soc. Jpn* **1995**, *68*, 2465−2469.

(11) Koike, T.; Gotoh, T.; Aoki, S.; Kimura, E.; Shiro, M. *Inorg. Chim. Acta* **1998**, *270*, 424−432.

(12) (a) Kimura, E.; Ikeda, T.; Shionoya, M. *Pure Appl. Chem.* **1997**, *69*, 2187−2195. (b) Kimura, E.; Ikeda, T.; Aoki, S.; Shionoya, M. *J. Biol. Inorg. Chem.* **1998**, *3*, 259−267.

(13) Aoki, S.; Honda, Y.; Kimura, E. *J. Am. Chem. Soc.* **1998**, *120*, 10018−10026.

(14) Aoki, S.; Sugimura, C.; Kimura, E. *J. Am. Chem. Soc.* **1998**, *120*, 10094−10102.

(15) Kimura, E.; Koike, T. *Chem. Commun.* **1998**, 1495−1500.

(16) Galas, D. J.; Schmitz, A. *Nucleic Acids Res.* **1978**, *5*, 3157−3170.

(17) Fox, K. R.; Warning, M. J. *Biochim. Biophys. Acta* **1987**, *909*, 145−155.

(18) Drew, H. R. *J. Mol. Biol.* **1984**, *176*, 535−557.

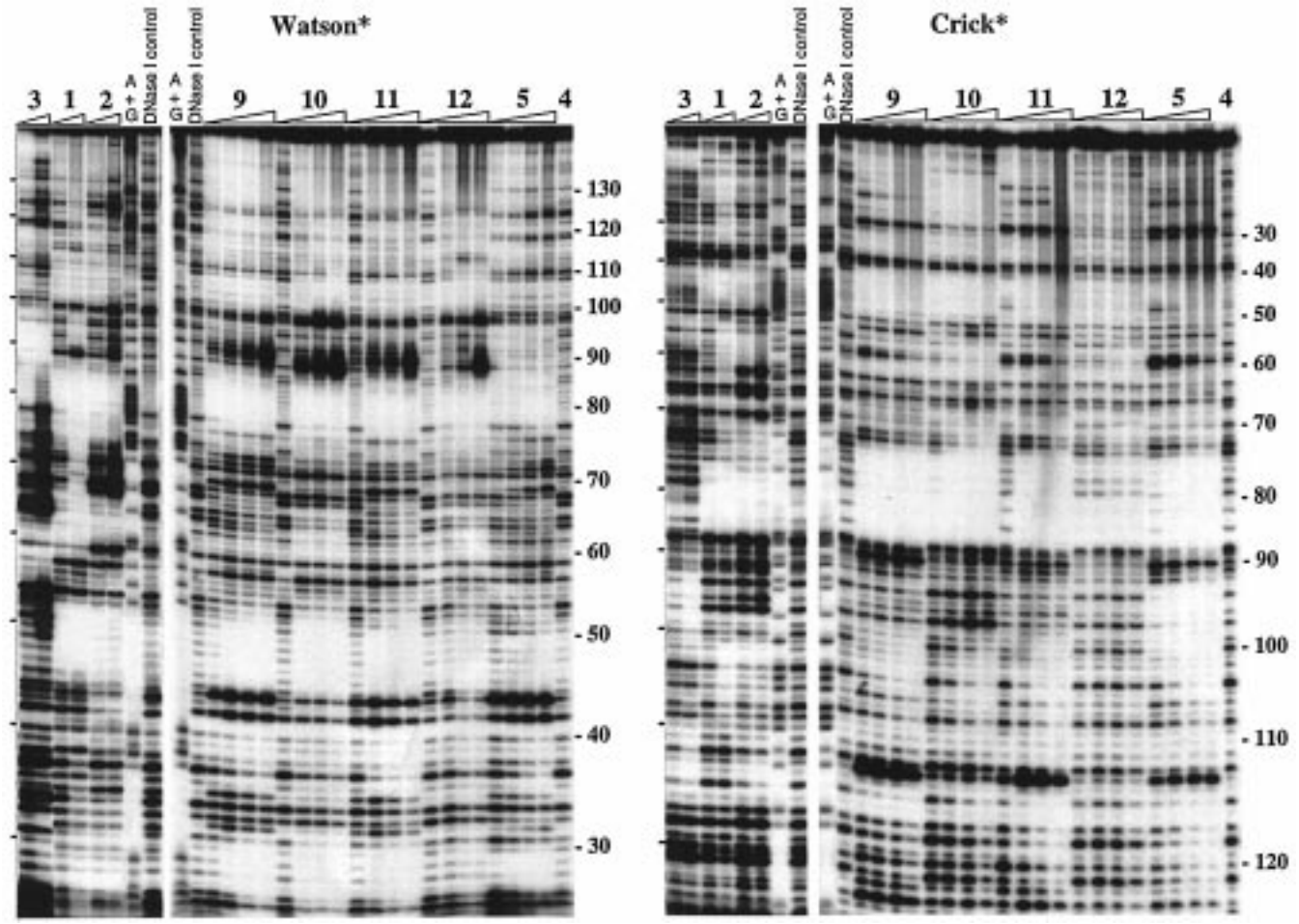

Figure 1. DNase I footprinting of 150 bp DNA in the presence of **1** (0.625 and 1.25 μM), **2** (1.25 and 2.5 μM), **3** (2.5 and 5 μM), **4** (100 μM), **5** (5, 7.5, 10, and 12.5 μM), **9** (30, 40, 50, and 60 μM), **10** (7.5, 10, 12.5, and 15 μM), **11** (20, 30, 40, and 50 μM), and **12** (5, 7.5, 10, and 12.5 μM). Hereafter, the asterisk indicates which strand bears the 5′-^{32}P label (Watson* = upper strand, Crick* = lower strand shown in Figure 2). The lane A+G represents the Maxam−Gilbert sequencing marker specific for A and G. The lane DNase I control represents DNA digested with DNase I without binders. The number at the side corresponds to the sequence number shown in Figure 2.

(**2**).[3,17] In the present study, we have added Zn^{2+}−cyclen derivatives appended with a quinoline group (Zn^{2+}−(4-quinolyl)-methyl-cyclen) **9**, two quinoline groups (Zn^{2+}−1,7-bis(4-quinolyl)methyl-cyclen) **10**, a naphthalene group (Zn^{2+}−(1-naphthyl)methyl-cyclen) **11**, and two naphthalene groups (Zn^{2+}−1,7-bis(1-naphthyl)methyl-cyclen) **12**.

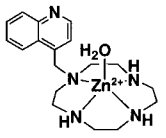

9

Zn^{2+}–(4-quinolyl)methyl-cyclen

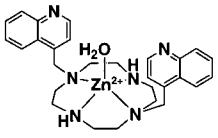

10

Zn^{2+}–1,7-bis((4-quinolyl)-methyl)-cyclen

11

Zn^{2+}–(1-naphthyl)methyl-cyclen

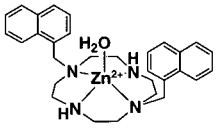

12

Zn^{2+}–1,7-bis((1-naphthyl)-methyl)-cyclen

Table 1. Comparison of the Conditional Affinity Constants log K(ZnL−dT$^-$) and log K(ZnL−dG)[a] at pH 8.0 and 25 °C

ZnL	log K(ZnL−dT$^-$)	log K(ZnL−dG)
4[b]	3.5	<2
5[c]	4.8	3.5
9[d]	4.3	2.4
10[d]	5.0	2.8
11[d]	4.2	2.4
12[e]	ND	ND

[a] K(ZnL−dT$^-$) = [ZnL−dT$^-$]/[ZnL][unbound dT] (M^{-1}), K(ZnL−dG) = [ZnL−dG]/[ZnL][unbound dG] (M^{-1}). The estimated error in the log K(ZnL−dT$^-$) and log K(ZnL−dG) values was ±5%. [b] From ref 8 with I = 0.10 ($NaClO_4$). [c] From ref 9 with I = 0.10 ($NaNO_3$). [d] With I = 0.05 ($NaNO_3$). [e] Due to insufficient solubility in aqueous solution, log K(ZnL−dT$^-$) and log K(ZnL−dG) values could not be determined.

Results and Discussion

New Aromatic Zn^{2+}−cyclen Derivatives 9−12. The new cyclen derivatives appended with aryl groups **9**−**12** were synthesized in a manner similar to that described for **5**[9] (see Experimental Section). The conditional affinity constants of **9**−**11** with dT$^-$ and dG, K(ZnL-dT$^-$) = [ZnL−dT$^-$]/[ZnL]-[unbound dT] (M^{-1}) and K(ZnL−dG) = [ZnL−dG]/[ZnL]-[unbound dG] (M^{-1}), respectively, were determined for pH 8 by almost the same potentiometric pH-titration method (at 25 °C with I = 0.05 ($NaNO_3$)) as previously reported.[9,11,19] The obtained K(ZnL−dT$^-$) values are around 10^4−10^5 M^{-1} (i.e.,

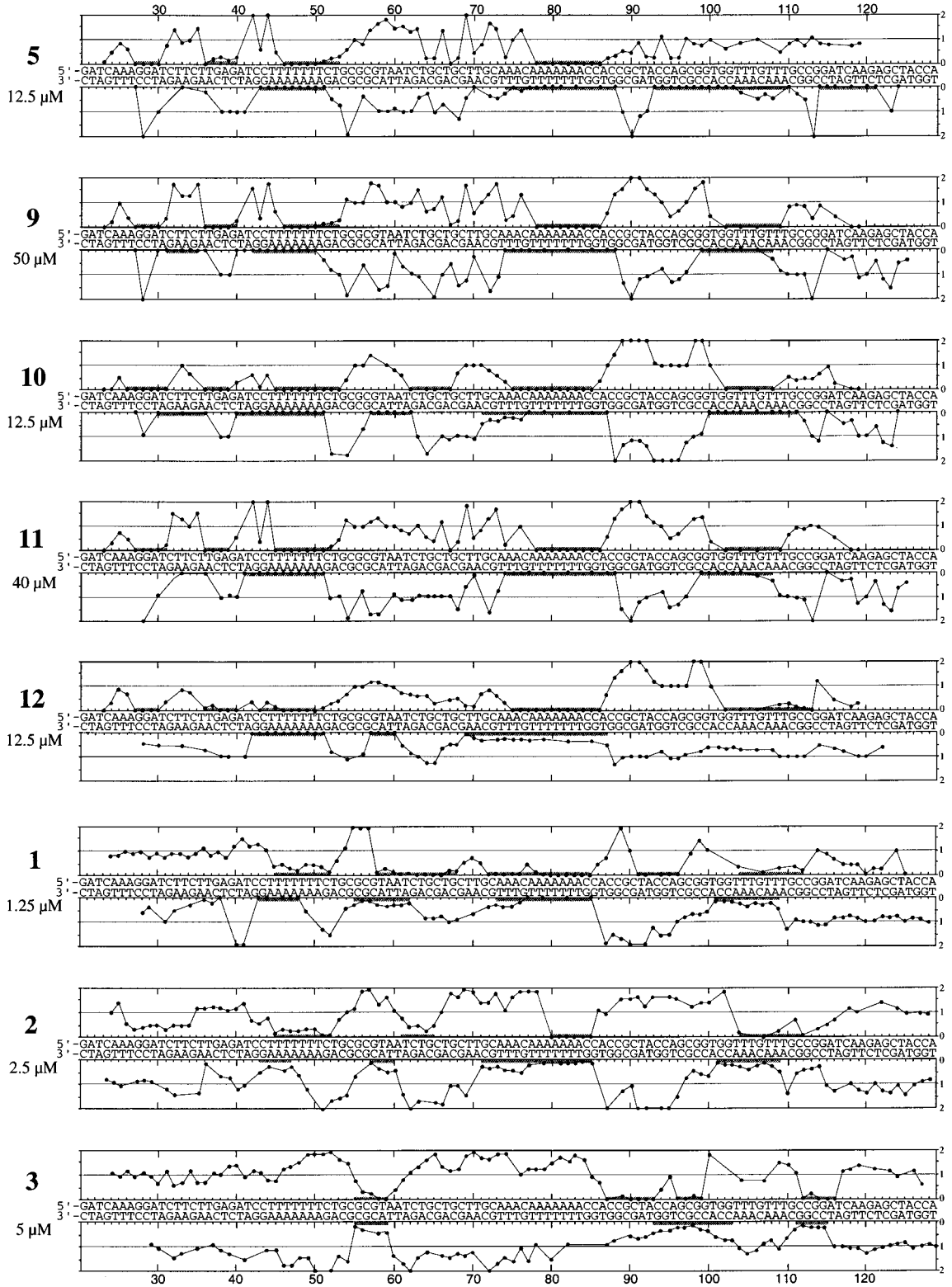

Figure 2. Differential DNase I cleavage plots in the presence of binders **5** (12.5 μM), **9** (50 μM), **10** (12.5 μM), **11** (40 μM), **12** (12.5 μM), **1** (1.25 μM), **2** (2.5 μM), and **3** (5.0 μM). The vertical scale corresponds to the ratio D/D_0, where D is the density of the band in the presence of a binder and D_0 in its absence.

dissociation constants K_d = ca. 10−100 μM), as summarized in Table 1. Due to insufficient solubility for the potentiometric pH-titration in aqueous solution, the K(ZnL−dT$^-$) and K(ZnL−dG) values for **12** could not be determined.

(19) A similiar method for the determination of conditional affinity constants for imide-deprotonated barbital complexes with Zn^{2+}−cyclen derivatives at pH 8 was previously reported: Fujioka, H.; Koike, T.; Yamada, N.: Kimura, E. *Heterocycles* **1996**, *42*, 775−787.

Identification of the Zn^{2+}−cyclen Derivatives Binding Sites on DNA (150bp). The binding sites of Zn^{2+}−cyclen derivatives **5**, **9**, **10**, **11**, and **12** (at concentrations 7.5−60 μM) on the 5′-^{32}P labeled DNA fragments from plasmid pUC19 (150 base pairs, the sequence is shown in Figure 2) have been analyzed first by DNase I footprinting method. The patterns of the DNase I digestion are shown in Figure 1 for the upper

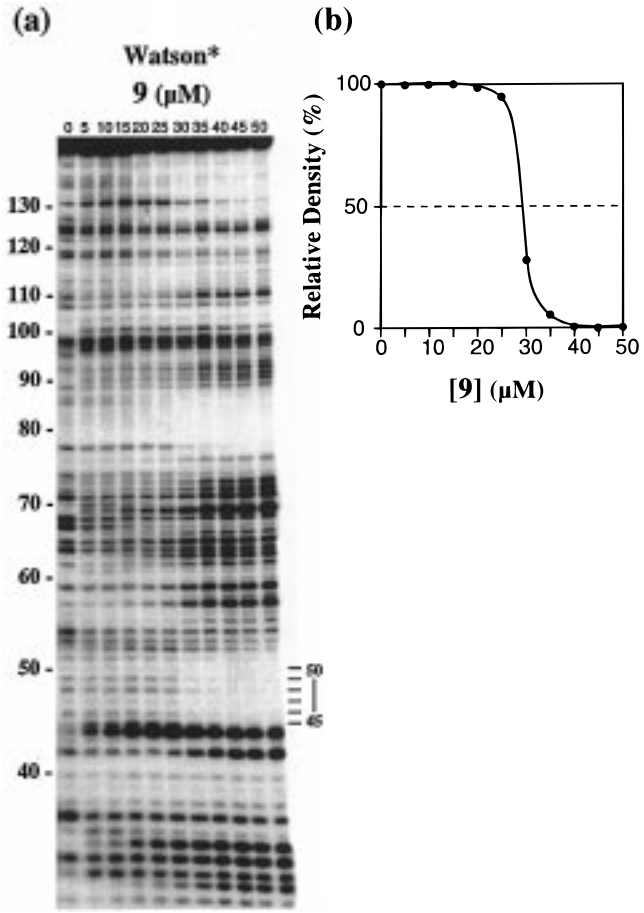

Figure 3. (a) DNase I footprinting titration with **9** (0−50 μM) on the 5′-^{32}P labeled Watson strand. (b) Footprinting titration plots of total density for the TpTpTpTpTpTpT moiety at 45−50. Relative density corresponds to the ratio D/D_0, where D is the total density of the six bands in the presence of **9** and D_0 in its absence.

Table 2. One-half the concentration values (IC_{50})[a] of Zn^{2+}−cyclen derivatives (**5**, **9**, **10**, **11**, and **12**) and minor groove binders (**1** and **2**) required to inhibit the DNase I hydrolysis at TpTpTpTpTpTpT (45−50) in the Watson strand

	IC_{50} (μM)
5	8
9	30
10	9
11	25
12	8
1	0.5
2	2

[a] The estimated error in the IC_{50} values was ±10%.

(Watson) and lower (Crick) strands. For comparison, minor groove binders distamycin A **1** (0.625−1.25 μM) and DAPI **2** (1.25−2.5 μM), which bind to AT-rich regions,[2,3,17] and a bis-intercalator echinomycin **3** (2.5−5 μM) that recognizes GC-rich regions[4] were also tested side by side.

It is immediately apparent that all of the protected regions with the Zn^{2+}−cyclen derivatives (**5**, **9**, **10**, **11**, and **12**) are similar to those recognized by distamycin A (**1**) and DAPI (**2**), but dissimilar to those by echinomycin (**3**). The interaction with GC-rich regions if any, on the other hand, would not be so strong as to hinder the DNase I attack. The acridine derivative **5** (e.g., 93−100 on the Crick strand) and bis-quinoline derivative **10** (e.g., 62−67 on the Watson strand) seemed to have minor interaction with GC-regions. Although there were some disparities between protected regions by the Zn^{2+}−cyclen derivatives and by the minor groove binders **1** and **2** (e.g., around 60), characteristically common protected sites are clearly discerned, located in the vicinity of the positions 48 and 80 on the Watson strand, and 80 and 105 on the Crick strand (see Figure 1). All of these common protected zones are associated with the homopolymeric AT-region in the DNA sequence, which appeared well defined in the differential cleavage plots (see Figure 2). Such protection was not observed with Zn^{2+}−cyclen **4** even at 100 μM concentration, implying that the aromatic rings are essential for the Zn^{2+}−cyclen part to interact with the DNA.

Binding affinities and specificities varied with the kind or number of aromatic rings appended to the Zn^{2+}−cyclen. Among those active species, **5**, **10**, and **12**, having higher log K(ZnL−dT$^-$) values at pH 8.0 (Table 1), showed the stronger binding with DNA. The evaluation came from the IC_{50} values, one-half of the concentration required to inhibit the DNase I hydrolysis at TpTpTpTpTpTpT (45−50) in the Watson strand, which were determined by the footprinting titration (see Figure 3) and the results summarized in Table 2. Although their IC_{50} values (8−30 μM) were not as small as those for 0.5 μM distamycin A (**1**) and 2 μM DAPI (**2**), we think that these values are significant for the starting prototype. Similar IC_{50} values were seen for **9** and **11** (25−30 μM), and for **10** and **12** (8−9 μM). The DNase I digestion patterns were somewhat different between **9** and **10** and between **11** and **12**. This may result from differences in the "single-stacking" binding mode by the single aromatic pendants vs the "double-stacking" binding mode by the double aromatic pendants.[20] The DNase I cleavage pattern of **5** was similar to those by **9** and **11**, although its IC_{50} value was higher and similar to those for **10** and **12**.

The footprinting technique using hydroxy radicals (e.g., by Fe^{2+}−EDTA) is often employed to elucidate the groove and sequence preference of DNA binding molecules.[2b,d,21] The footprinting with Fe^{2+}−EDTA ([Fe^{2+}] = 10 μM and [EDTA] = 20 μM), which gave anticipated DNA cleavage patterns in the absence and presence of distamycin A (**1**), was carried out in the presence of the Zn^{2+}−cyclen derivatives (0−100 μM). However, little cleavage of DNA occurred with increasing concentrations of Zn^{2+}−cyclen derivatives, which may result from the ligand displacement between Fe^{2+} and Zn^{2+}.

Effects of Zn^{2+}, Cu^{2+}, and Ni^{2+} Ions on the Cyclen Binding to DNA. Zn^{2+} is essential in the interaction of cyclen derivatives with T.[8−15] In the absence of Zn^{2+}, these ligands did not protect the AT-rich regions, as demonstrated by the DNase I footprinting experiment with **9** (50 μM) (see Figure 4). Upon the addition of increasing concentrations of Zn^{2+}, the protection of the AT-rich regions emerged (the vicinity of 48 and 80 on the Watson strand). On the other hand, other divalent metal ions such as Cu^{2+} or Ni^{2+} were not effective at all, although these ions form more stable 1:1 complexes with cyclen than Zn^{2+}.[22] Moreover, Zn^{2+} (up to 50 μM) alone did not protect DNA from the DNase I hydrolysis. These observations are compatible with our prediction based on the T-binding by the Zn^{2+}−cyclen derivatives. We observed that Cu^{2+}− and Ni^{2+}−cyclen derivatives did not interact with deoxythymidine in the physiological pH.

(20) Significantly larger complexation constants with dT$^-$ (or U$^-$) (see Table 1) and the ^{1}H NMR data (e.g., a large upfield shift of thymine H(6) in dT$^-$−**10** (δ 7.12 at pD 8.5) from uncomplexed dT$^-$ (δ 7.50 at pD >12)) suggest that the aromatic rings in **10** and **12** act as bis-intercalators to sandwich the thymine group.

(21) (a) Lokey, R. S.; Kwok, Y.; Guelev, V.; Pursell, C. J.; Hurley, L. H.; Iverson, B. L. *J. Am. Chem. Soc.* **1997**, *119*, 7202−7210. (b) Tullius, T. D. *Science* **1988**, *332*, 663−664.

(22) (a) Kimura, E. *J. Coord. Chem.* **1986**, *15*, 1−28. (b) Kodama, M.; Kimura, E. *J. Chem. Soc., Chem. Commun.* **1975**, 326−327. (c) Kodama, M.; Kimura, E. *J. Chem. Soc., Dalton. Trans.* **1977**, 2269−2276.

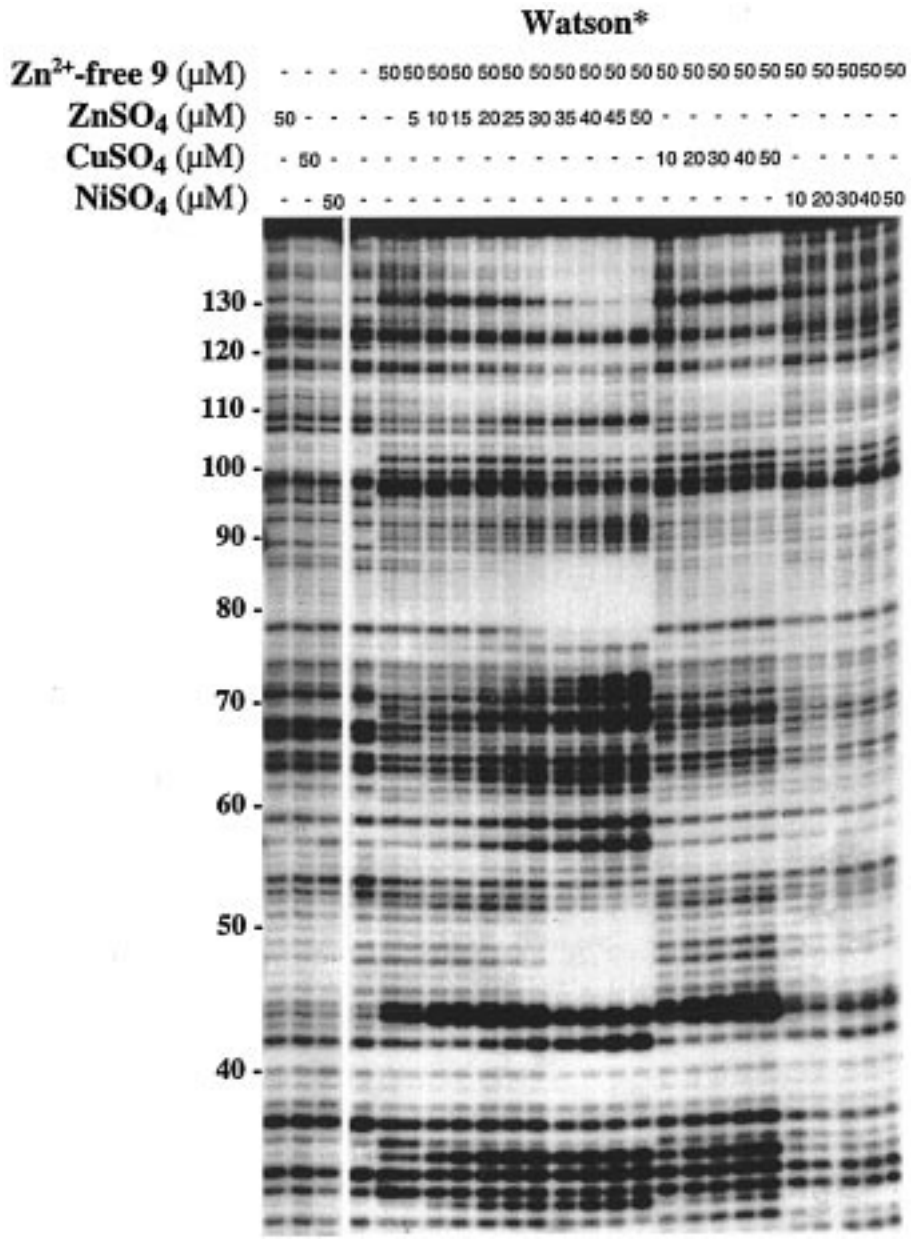

Figure 4. Effect of Zn^{2+} (0−50 μM), Cu^{2+} (0−50 μM), and Ni^{2+} (0−50 μM) on binding of Zn^{2+}−free ligand of **9** (50 μM) to DNA (5′-^{32}P labeled Watson strand).

Inhibition of the DNA Binding of Zn^{2+}−cyclen Derivatives by Thiolate Anion (Captopril). A thiolate anion strongly binds to Zn^{2+}−cyclen at the fifth coordination site, as exemplified by captopril complexation (see **13**) with log *K* of 7.0 at 25 °C.[23] When captopril was added to 50 μM of **9**, the protection of AT-rich regions by **9** was dose-dependently decreased (see Figure 5). This implies that the fifth coordination site of the Zn^{2+}−cyclen should be available for the effective binding with the double-stranded DNA.

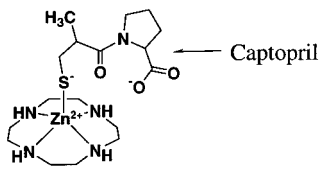

13

Further Information on the Zn^{2+}−cyclen Derivatives Binding to DNA. To more precisely characterize the AT-rich region protected by the Zn^{2+}−cyclen derivatives, we have studied the DNA footprinting by micrococcal nuclease, an enzyme that cuts DNA more efficiently at pA and pT bonds than at pG and pC bonds.[3a,17,18] Micrococcal nuclease is known to recognize single-stranded sites in the DNA without too much interference from the opposing strand.[18] This enzyme thus might be extremely useful for comparing the AT recognition mode of the Zn^{2+}−cyclen derivatives with those of distamycin A and DAPI.

Indeed, the micrococcal nuclease footprinting (see Figure 6) illustrated the interaction of Zn^{2+}−cyclen derivatives with the AT sites with more insight than the above DNase I footprinting (see Figure 1). Thus, *Zn^{2+}−cyclen derivatives **5**, **9**, **10**, **11**, and **12** protected almost all of the pT bonds from the micrococcal nuclease hydrolysis. On the other hand, they did not protect the pairing pA bonds, resulting in remarkable hydrolysis, especially at homopolymeric A regions* (e.g., the positions 78−83 on the Watson strand and 45−50 and 103−109 on the Crick strand). These results clearly indicate that **5**, **9**, **10**, **11**, and **12**

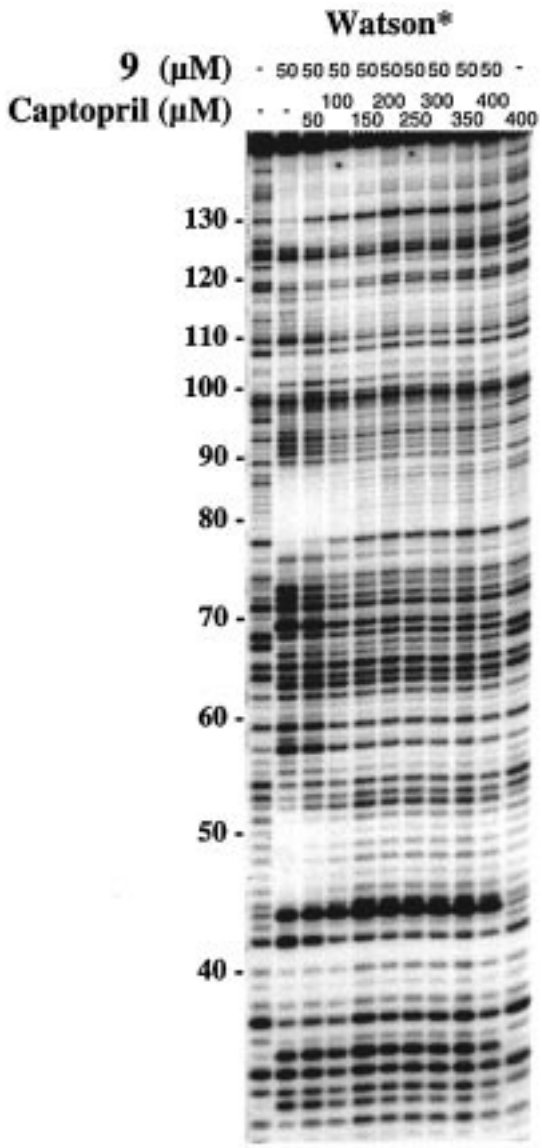

Figure 5. Effect of a thiolate anion, captopril (0−400 μM) on **9** (50 μM) binding to DNA (5′-^{32}P labeled Watson strand).

selectively bind to the thymine groups to melt the A−T base pair and that the separated A partners became subject to the strong digestion by micrococcal nuclease (see Figure 7). The released strand, -pApApA-, from the homopolymeric AT-rich regions was extremely vulnerable.

In the first DNase I footprinting (see Figure 1), the T and A partners together were protected in the homopolymeric AT-rich regions. DNase I tends to cut the firm double-stranded region rather than the breathing single-stranded region because it recognizes the minor groove of DNA and binds across two strands.[18] Hence, the observed protection of homopolymeric AT regions may simply show the perturbation of the double helical structure by the Zn^{2+}−cyclen derivatives. The exclusive binding of the Zn^{2+}−cyclen derivatives to T was not concluded from the DNase I footprinting.

For distamycin A (**1**) and DAPI (**2**), the micrococcal nuclease footprinting clearly showed that pT and pA pairing together in the homopolymeric AT regions were well-protected from hydrolysis (e.g., the vicinity of the positions 48, 80 on both strands). This fact well reflects that the minor groove binders simultaneously bind to both A and T in the AT minor groove to stabilize the double helix as depicted in Scheme 1. Moreover, these reagents need three or more consecutive A−T base pairs to bind.[2,3] By comparison, the Zn^{2+}−cyclen derivatives can recognize all of the thymine groups in the AT sites.

Competition between Distamycin A (1) and 9 for AT-regions in DNA. To see that distamycin A (**1**) and **9** share common AT-rich region in equilibrium, a competitive binding study was performed. First, to DNA (5′-^{32}P labeled Watson strand) preincubated with 60 μM of **9** was added **1** (0−10 μM), which was then digested with micrococcal nuclease (see Figure 8a). It was evident that the initial **9**-controlled footprinting pattern at the T region (e.g., positions 45−50) and the A region (e.g., positions 78−83) were dose-dependently changed to the **1**-controlled patterns. Conversely, to DNA preincubated with 5 μM of **1** was added **9** (0−60 μM), which showed that the initial **1**-controlled footprinting patterns were gradually replaced by the **9**-controlled patterns (see Figure 8b). Taking these results together, it is concluded that distamycin A (**1**) and the Zn^{2+}−cyclen complex **9** reversibly compete for common AT regions. The Zn^{2+}−cyclen derivatives would bind to thymine via the minor groove of the AT region.

Concluding Remarks

By the DNase I footprinting assay, zinc(II)−macrocyclic tetraamine complexes appended with aromatic pendants **9**−**12**, have been proven to selectively bind to AT-rich regions of double-stranded DNA (150 bp). The regions were almost overlapped with the sites recognized by conventional minor groove binders, distamycin A (**1**) and DAPI (**2**). The Zn^{2+}−cyclen appended with double pendants **10** and **12** showed higher affinity to the AT-rich regions than those with single pendant counterparts **9** and **11**, as measured by the IC_{50} values. The DNase I cleavage pattern was somewhat different for the double pendants and the single pendant systems. The Zn^{2+}−cyclen appended with single acridine-pendant **5** showed an affinity as high as **10** and **12**, and a DNase I cleavage pattern similar to that of **9** and **11**. Zn^{2+} is an essential metal ion for the recognition of AT-rich regions, which could not be replaced by other metal ions such as Cu^{2+} or Ni^{2+}. The vacant fifth coordination site of the Zn^{2+}−cyclen is essential, as demonstrated by the strong inhibition of the SH-containing captopril.

The footprinting by micrococcal nuclease, which tends to cut pA and pT more than pC and pG and has a specific ability to nick the transiently melted DNA, revealed the fundamentally different interaction modes by the Zn^{2+}−cyclen derivatives and minor groove binders distamycin A (**1**) and DAPI (**2**). It was shown that almost all the T's in double-stranded DNA were recognized by the Zn^{2+}−cyclen derivatives, resulting in the protection of those pT bonds. On the other hand, the pairing pA's were strongly hydrolyzed. It is concluded that the Zn^{2+}−cyclen derivatives broke into the hydrogen bonds of A−T base pairs to bind to T, especially at homopolymeric AT-regions. The resulting single-stranded A region thus became exposed and came under heavy attack by the nuclease. By contrast, **1** and **2** interacted with A and T simultaneously in the same AT regions to protect both A and T from the micrococcal nuclease hydrolysis. Finally, it was demonstrated that **1** and **9** reversibly compete for common AT regions. Such T-recognizing properties of the Zn^{2+}−cyclen derivatives will find useful biochemical and medicinal applications.[24]

Experimental Section

General Information. All reagents and solvents used were purchased at the highest commercial quality and used without purification.

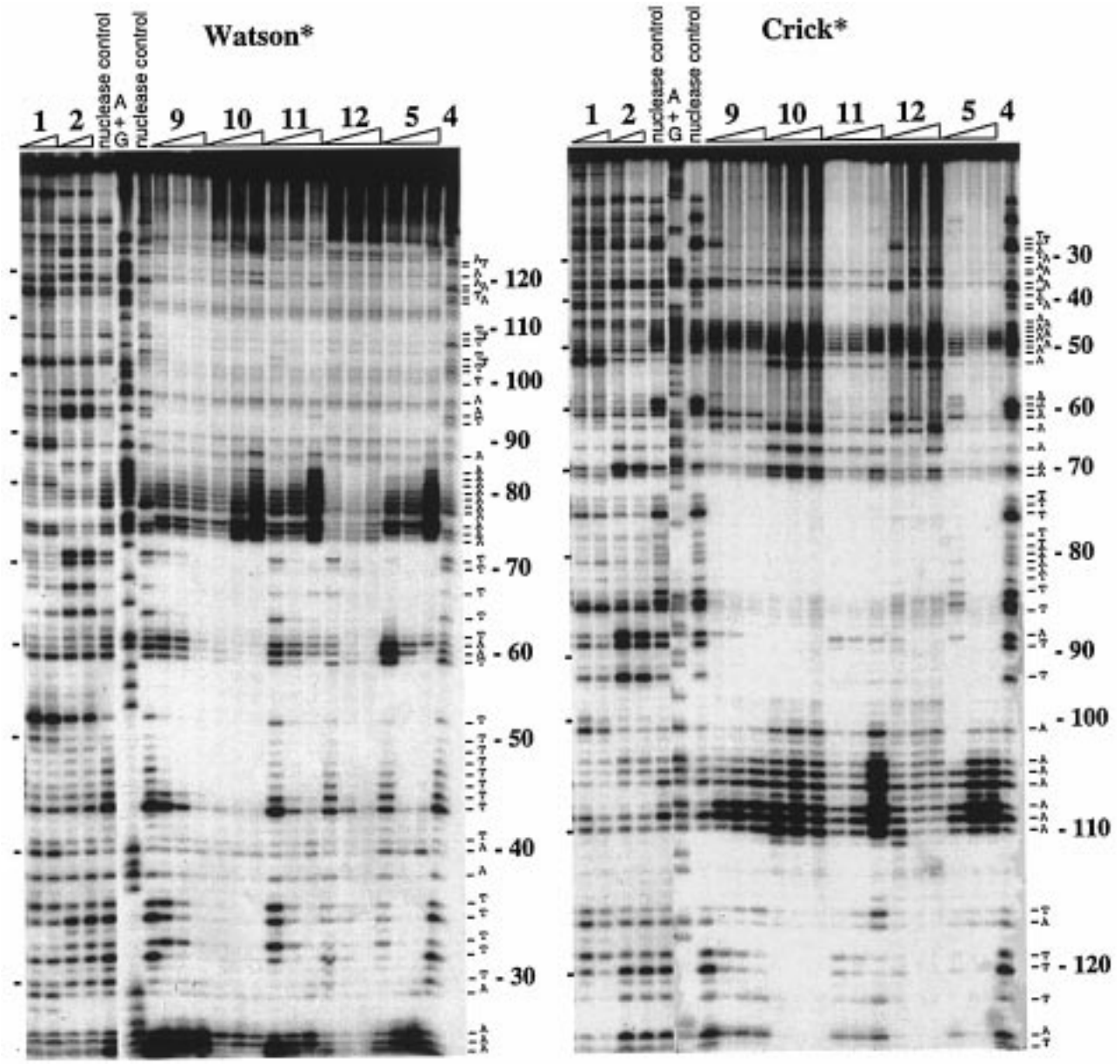

Figure 6. Micrococcal nuclease footprinting in the presence of **1** (5 and 10 μM), **2** (5 and 10 μM), **4** (100 μM), **5** (10, 20, and 30 μM), **9** (40, 60, and 80 μM), **10** (10, 20, and 30 μM), **11** (20, 40, and 60 μM), and **12** (5, 10, and 15 μM). The lane nuclease control represents DNA digestion without binders.

Aqueous solutions of 10 mM distamycin A (Sigma) and 10 mM DAPI (4,6-diamidine-2-phenylindole) (Sigma) were prepared using deionized and distilled water and stored at −20 °C. A stock solution of 3 mM echinomycin (Sigma) in dimethyl sulfoxide was prepared and stored at −20 °C. Concentrations of distamycin A, DAPI, and echinomycin in aqueous solution were determined spectrophotometrically (ϵ_{303} = 34 000 M^{-1} cm^{-1} for distamycin A,[2h] ϵ_{342} = 23 000 for DAPI,[3d] ϵ_{325} = 11 500 for echinomycin[4d]). Calf thymus DNA (Sigma) was dissolved in water, sonicated, and filtered before use. Its concentration was determined spectrophotometrically (ϵ_{253} = 6600 M^{-1} cm^{-1}).[25] DNase I (Takara Shuzo Co.) and micrococcal nuclease (Worthington Biochemical Corporation) were diluted to 0.03 unit/μL in aqueous solution containing 2.5 mM $CaCl_2$ and 5 mM $MgCl_2$, and stocked at −20 °C. UV spectra were recorded on a Hitachi U-3500 spectrophotometer at 25 °C. IR spectra were recorded on a Shimadzu FTIR-4200 spectrophotometer at room temperature. ^{1}H(500 MHz), and ^{13}C(125 MHz) NMR spectra at 35 °C were recorded on a JEOL LA500 spectrometer. 3-(Trimethylsilyl)propionic-2,2,3,3-d_4 acid sodium salt in D_2O and tetramethylsilane in DMSO-d_6 were used as internal references for NMR measurements. Elemental analysis was performed on a Perkin-Elmer CHN Analyzer 2400. Silica gel column chromatography was performed using Fuji Silysia Chemical FL-100D.

Synthesis of Zn^{2+}−(4-Quinolyl)methyl-cyclen, 9·$(NO_3)_2$. An acetonitrile solution (120 mL) of 4-(chloromethyl)-quinoline (774 mg, 4.36 mmol) and 1,4,7,10-tetraazacyclododecane (1.50 g, 8.71 mmol) was stirred for 12 h at 70 °C. After evaporation of the solvent, the residue was purified by silica gel column chromatography (CH_2Cl_2/MeOH/28% aqueous NH_3 = 10:1:0.1) followed by crystallization from aqueous 48% HBr/MeOH to obtain colorless needles of (4-quinolyl)-methyl-cyclen·4HBr·$2H_2O$ (1.11 g, 45% yield). IR (KBr pellet) 3425, 3005, 2722, 1599, 1441, 1415, 1291, 1221, 1074, 831, 527 cm^{-1}. ^{1}H

(23) Koike, T.; Takamura, M.; Kimura, E. *J. Am. Chem. Soc.* **1994**, *116*, 8443−8449.

(24) Our preliminary experiments showed that the Zn^{2+}−cyclen complexes selectively bound to a TATA box, AT-rich element in the promoter region required for proper initiation of gene transcription by RNA polymerase II, which then inhibited binding of the transcription factor, TFIID, to the TATA box. We also found antimicrobial activities of Zn^{2+}−cyclen complexes, which will be reported elsewhere.

(25) Wells, R. D.; Larson, J. E.; Grant, R. C.; Shortle, B. E.; Cantor, C. R. *J. Mol. Biol.* **1970**, *54*, 465−497.

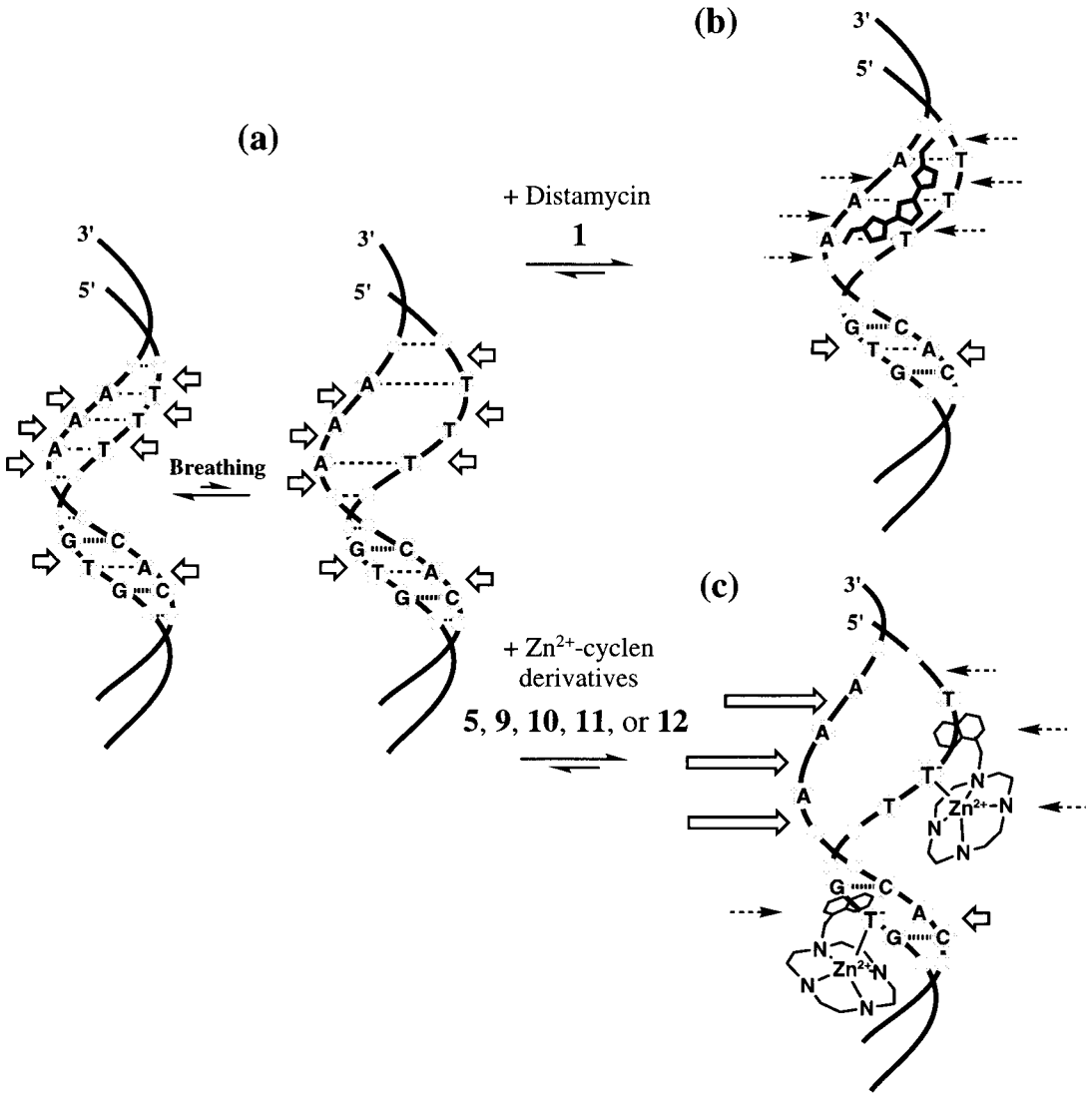

Figure 7. Schematic representation of the micrococcal nuclease attack to (a) breathing double-stranded DNA (b) distamycin-bound DNA, and (c) Zn^{2+}−cyclen derivative-bound DNA. Arrows and dashed arrows, respectively, indicate successful and failed hydrolysis by micrococcal nuclease.

NMR (D_2O, 55 °C) δ 3.04 (4H, t, J = 5.1 Hz, NCH_2), 3.08 (4H, t, J = 5.1 Hz, NCH_2), 3.22 (4H, t, J = 4.9 Hz, NCH_2), 3.31 (4H, t, J = 4.9 Hz, NCH_2), 4.63 (2H, s, $ArCH_2$), 8.03 (1H, m, ArH), 8.10 (1H, d, J = 5.5 Hz, ArH), 8.19 (1H, m, ArH), 8.28 (1H, d, J = 8.5 Hz, ArH), 8.44 (1H, d, J = 9.5 Hz, ArH), 9.10 (1H, d, J = 5.5 Hz, ArH). ^{13}C NMR (D_2O) δ 44.5, 45.3, 47.5, 51.6, 56.4, 124.2, 124.4, 127.4, 130.9, 133.5, 138.1, 140.2, 146.3, 159.0. Anal. Calcd for $C_{18}H_{35}N_5O_2Br_4$: C, 32.1; H, 5.2; N, 10.4. Found: C, 32.2; H, 5.3; N, 10.3.

The solution pH of (4-quinolyl)methyl-cyclen·4HBr·$2H_2O$ (600 mg, 0.891 mmol) in 10 mL of H_2O was adjusted to 12 with 5 M NaOH. The alkaline solution was extracted with CH_2Cl_2 (50 mL × 8) and then the organic solvent was evaporated. An EtOH solution (10 mL) of the obtained acid-free ligand and $Zn(NO_3)_2$·$6H_2O$ (280 mg, 0.941 mmol) was stirred at room temperature for 1 h. After evaporation of the solvent, the residue was crystallized from H_2O/EtOH to obtain colorless needles of **9**·$(NO_3)_2$ (357 mg, 80% yield). IR (KBr pellet) 3206, 1468, 1385 (NO_3^-), 1302, 1086, 978, 775 cm^{-1}. ^1H NMR (D_2O) δ 2.80−2.92 (8H, m, NCH_2), 2.95−3.10 (6H, m, NCH_2), 3.20−3.35 (2H, m, NCH_2), 4.57 (2H, s, $ArCH_2$), 7.63 (1H, d, J = 4.5 Hz, ArH), 7.80 (1H, dd, J = 6.5 and 8.5 Hz, ArH), 7.93 (1H, dd, J = 6.5 and 8.5 Hz, ArH), 8.17 (1H, d, J = 8.5 Hz, ArH), 8.28 (1H, d, J = 8.5 Hz, ArH), 8.90 (1H, d, J = 4.5 Hz, ArH). ^{13}C NMR (D_2O) δ 45.3, 46.5, 47.6, 52.8, 53.6, 126.5, 127.1, 130.68, 130.73, 131.4, 133.3, 142.4, 149.9, 152.2. Anal. Calcd for $C_{18}H_{27}N_7O_6Zn$: C, 43.0; H, 5.4; N, 19.5. Found: C, 43.1; H, 5.5; N, 19.6.

Synthesis of Zn^{2+}−1,7-Bis(4-quinolyl)methyl-cyclen, 10·$(NO_3)_2$·H_2O. An acetonitrile solution (120 mL) of 4-(chloromethyl)-quinoline (2.40 g, 13.5 mmol), K_2CO_3 (1.90 g, 13.7 mmol), and 1,7-bis-(diethoxyphosphoryl)-1,4,7,10-tetraazacyclododecane (2.00 g, 4.5 mmol)[26] was refluxed for 1 day. After removal of inorganic salts, the solvent was evaporated. The residue was purified by silica gel column chromatography (eluent, CH_2Cl_2/MeOH = 25:1). After evaporation of the solvent, MeOH (15 mL) and 36% aqueous HCl (5 mL) were added. The reaction mixture was stirred at 60 °C for 12 h. After evaporation of the solvent, the residue was dissolved in H_2O (20 mL) and the solution pH was adjusted to 12 with 5 M NaOH. The alkaline solution was extracted with CH_2CH_2 (100 mL × 5) and the solvent was evaporated. The residue was crystallized from 48% aqueous HBr/MeOH to obtain 1,7-bis(4-quinolyl)methyl-cyclen·4HBr·$2H_2O$ as colorless prisms (1.33 g, 36% yield). IR (KBr pellet) 3351, 2635, 1599, 1389, 1343, 1051, 822, 612 cm^{-1}. ^1H NMR (D_2O) δ 3.25 (8H, t, J = 5.0 Hz, NCH_2), 3.44 (8H, t, J = 5.0 Hz, NCH_2), 4.84 (4H, s, $ArCH_2$), 8.07 (2H, dd, J = 6.5 and 8.5 Hz, ArH), 8.15 (2H, d, J = 5.5 Hz, ArH) 8.22 (2H, dd, J = 6.5 and 8.5 Hz, ArH), 8.31 (2H, d, J = 8.5 Hz, ArH), 8.52 (2H, d, J = 8.5 Hz, ArH), 9.15 (2H, d, J = 5.5 Hz, ArH). ^{13}C NMR (D_2O) δ 46.1, 50.7, 55.6, 124.52, 124.54, 127.5, 131.1, 133.4, 137.9, 140.7, 146.4, 157.6. Anal. Calcd for $C_{28}H_{42}N_6O_2Br_4$: C, 41.3; H, 5.2; N, 10.3. Found: C, 41.3; H, 5.3; N, 10.2.

(26) Dumont, A.; Jacques, V.; Desreux, J. F. *Tetrahedron Lett.* **1994**, *35*, 3707−3710.

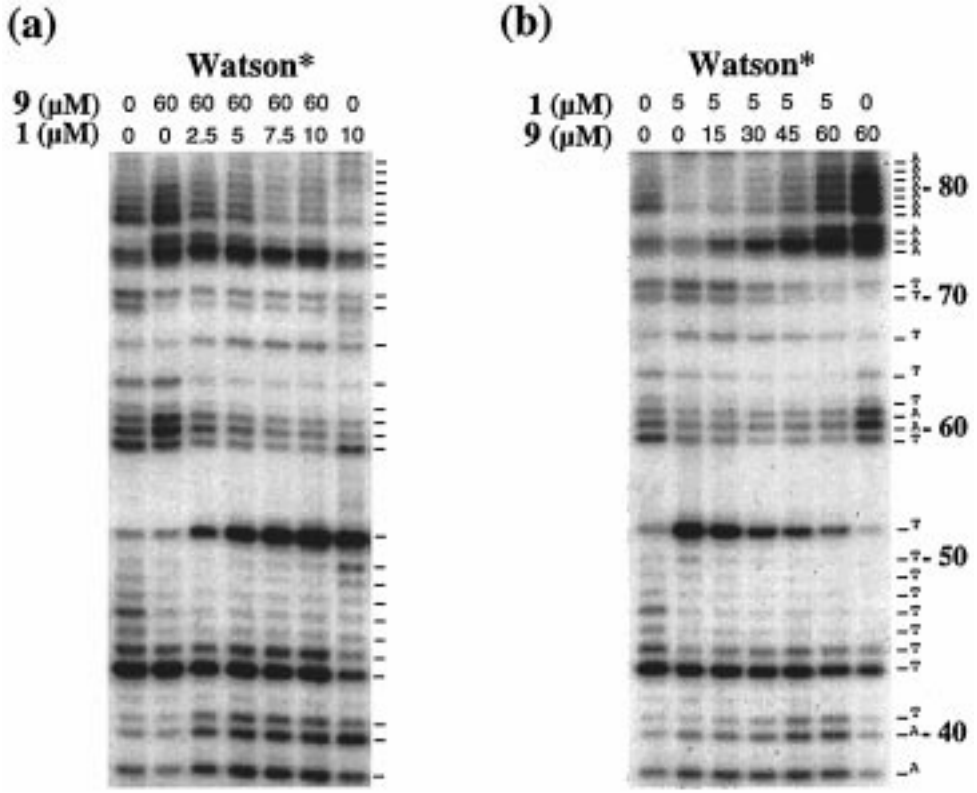

Figure 8. Micrococcal nuclease footprinting assay demonstrating displacement of DNA binding (5′-^{32}P labeled Watson strand): (a) 60 μM **9** by 0−10 μM distamycin A (**1**), (b) **5** μM distamycin A (**1**) by 0−60 μM **9**.

Zinc(II) complex **10**·$(NO_3)_2$·H_2O as colorless prisms was obtained in 70% yield by almost the same method as used for **9** except using the H_2O/MeOH for its crystallization. IR (KBr pellet) 3223, 1491, 1385 (NO_3-), 1287, 1092, 772 cm^{-1}. ^{1}H NMR (D_2O): δ 2.86−2.91 (4H, m, NCH_2), 2.97−3.05 (4H, m, NCH_2), 3.00−3.15 (4H, m, NCH_2), 3.35−3.41 (4H, m, NCH_2), 4.60 (4H, s, $ArCH_2$), 7.82 (2H,d, J = 4.5 Hz, ArH), 7.84 (2H, dd, J = 6.5 and 8.5 Hz, ArH), 7.96 (2H, dd, J = 6.5 and 8.5 Hz, ArH), 8.19 (2H, d, J = 8.5 Hz, ArH), 8.29 (2H, d, J = 8.5 Hz, ArH), 8.94 (2H, d, J = 4.5 Hz, ArH). ^{13}C NMR (DMSO-d_6) δ 43.0, 49.3, 50.6, 123.75, 123.84, 127.0, 127.6, 129.3, 129.9, 138.3, 148.1, 149.8. Anal. Calcd for $C_{28}H_{36}N_8O_7Zn$: C, 50.8; H, 5.5; N, 16.9. Found: C, 51.2; H, 5.6; N, 16.9.

Synthesis of Zn^{2+}−(1-Naphthyl)methyl-cyclen, 11·$(NO_3)_2$. An acetonitrile solution (60 mL) of 1-(chloromethyl)-naphthalene (934 mg, 5.29 mmol) and 1,4,7-tris(*tert*-butyloxycarbonyl)-1,4,7,10-tetraazacyclododecane[27] (1.00 g, 2.12 mmol) was refluxed in the presence of K_2CO_3 (730 mg, 5.29 mmol) for 1 day. After removal of the inorganic salts, the solvent was evaporated. The residue was purified by silica gel column chromatography (eluent, CH_2Cl_2/MeOH = 50:1). After evaporation of the solvent, the residue was dissolved in EtOH (10 mL), and then 48% aqueous HBr (2 mL) was added. The reaction mixture was stirred for 12 h at room temperature. After evaporation of the solvent, the residue was crystallized from 48% aqueous HBr/MeOH to obtain colorless needles of (1-naphthyl)methyl-cyclen·3HBr·H_2O (0.742 mg, 61% yield). IR (KBr pellet) 2953, 2705, 1597, 1443, 1069, 781 cm^{-1}. ^{1}H NMR (D_2O) δ 2.92 (4H, br, NCH_2), 3.02−3.04 (8H, m, NCH_2), 3.12 (4H, br, NCH_2), 4.35 (2H, s, $ArCH_2$), 7.58−7.67 (3H, m, ArH), 7.71 (1H, t, J = 7.5 Hz, ArH), 8.02 (1H, d, J = 8.0 Hz, ArH) 8.07−8.09 (2H, m, ArH). ^{13}C NMR (D_2O) δ 44.8, 45.2, 47.0, 52.5, 58.9, 125.5, 128.9, 129.5, 130.2, 132.4, 132.5, 132.6, 134.1, 134.4, 136.8. Anal. Calcd for $C_{19}H_{33}N_4OBr_3$: C, 39.8; H, 5.8; N, 9.8. Found: C, 40.0; H, 5.9; N, 9.8.

Zinc(II) complex **11**·$(NO_3)_2$ as colorless prisms was obtained in 53% yield by almost the same method as that used for **9**. IR (KBr pellet) 3204, 1495, 1385 (NO_3^-), 1092, 980, 791 cm^{-1}. ^{1}H NMR (D_2O) δ 2.59−2.64 (2H, m, NCH_2), 2.76−2.88 (6H, m, NCH_2), 2.93−3.04 (6H, m, NCH_2), 3.20−3.26 (2H, m, NCH_2), 4.48 (2H, s, $ArCH_2$), 7.58−7.71 (4H, m, ArH), 8.02−8.05 (2H, m, ArH), 8.21 (1H, d, J = 8.5 Hz, ArH). ^{13}C NMR (D_2O) δ 45.3, 46.5, 47.5, 52.7, 54.5, 126.2, 128.2, 129.1, 129.9, 131.2, 132.0, 132.4, 133.5, 135.5, 136.6. Anal. Calcd for $C_{19}H_{28}N_6O_6Zn$: C, 45.5; H, 5.6; N, 16.8. Found: C, 45.8; H, 5.6; N, 16.5.

Synthesis of Zn^{2+}−1,7-Bis(1-naphthyl)methyl-cyclen, 12·$(NO_3)_2$. 1,7-Bis(1-naphthyl)methyl-cyclen·2HBr·H_2O as colorless prisms was obtained in 40.0% yield by almost the same method as that used for **10**. IR (KBr pellet) 3436, 2953, 2768, 1466, 1395, 783 cm^{-1}. ^{1}H NMR (DMSO-d_6) δ 2.92 (8H, br, NCH_2), 3.21 (8H, br, NCH_2), 4.32 (4H, s, $ArCH_2$), 7.56−7.67 (8H, m, ArH), 7.95 (2H, d, J = 7.9 Hz, ArH), 8.01 (2H, d, J = 7.6 Hz, ArH), 8.26 (2H, d, J = 8.6 Hz, ArH). ^{13}C NMR (DMSO-d_6) δ 42.5, 47.8, 52.8, 123.4, 125.4, 125.7, 126.5, 127.98, 128.05, 128.8, 132.0, 132.1, 133.5. Anal. Calcd for $C_{30}H_{40}N_4OBr_2$: C, 57.0; H, 6.4; N, 8.9. Found: C, 57.1; H, 6.3; N, 8.9.

Zinc(II) complex **12**·$(NO_3)_2$ was obtained as colorless prisms in 68.0% yield by almost the same method as that used for **9** except using the H_2O/CH_3CN for its crystallization. IR (KBr pellet) 3189, 1945, 1385 (NO_3-), 1096, 1013, 785 cm^{-1}. ^{1}H NMR (DMSO-d_6) δ 2.50−2.57 (4H, m, NCH_2), 2.74−2.87 (4H, m, NCH_2), 2.91−3.01 (4H, m, NCH_2), 3.05−3.20 (4H, m, NCH_2), 4.48 (4H, s, $ArCH_2$), 7.58−7.70 (8H, m, ArH), 8.00−8.03 (4H, m, ArH), 8.28 (2H, d, J = 8.3 Hz, ArH). ^{13}C NMR (DMSO-d_6) δ 43.0, 49.0, 51.1, 123.6, 125.1, 125.8, 126.6, 128.7, 128.9, 129.0, 130.4, 132.6, 133.6. Anal. Calcd for $C_{30}H_{36}N_6O_6Zn$: C, 56.1; H, 5.7; N, 13.1. Found: C, 56.4; H, 5.8; N12.7.

Preparation of 5′-Labeled DNA Fragments. The 150 bp DNA fragments (pUC19 sequence from 1881 to 2030 (AT-rich region) was arbitrarily selected) was amplified by PCR using pUC19 as a template and two 20 mer primers (5′GCGTCAGACCCCGTAGAAAA3′ and 5′AGTTACCTTCGGAAAAAGAG3′) obtained from Amersham Pharmacia Biotech. The 5′-end of either primer (Watson or Crick strand) was 5′-^{32}P labeled with T4 polynucleotide kinase and [γ-^{32}P] ATP. The amplified DNA fragments were purified by nondenatured polyacrylamide gel electrophoresis.

(27) Kimura, E.; Aoki, S.; Koike, T.; Shiro, M. *J. Am. Chem. Soc.* **1997**, *119*, 3068−3076.

DNase I and Micrococcal Nuclease Footprintings. The 5′-^{32}P labeled 150 bp DNA fragment (10 000 cpm) and sonicated calf thymus DNA (100 μM base) were incubated with a testing Zn^{2+}−cyclen complex in 50 μL of 10 mM EPPS (pH 8.0) at 25 °C for an hour. Then 0.09 unit of DNase I or micrococcal nuclease was added and incubated for 3 min at room temperature. Digestion was quenched by the addition of 10 μL solution containing 50 mM EDTA, 0.5%(w/v) sodium dodecyl sulfate (SDS), 1.8 M sodium acetate, and 10 μg yeast tRNA. The cleaved DNA was ethanol precipitated, dried, and dissolved in 3 μL of 95%(v/v) formamide/H_2O containing 0.05%(w/v) bromophenol blue, 0.05%(w/v) xylene cyanol, and 20 mM EDTA. They were heated at 95 °C for 10 min and loaded onto denatured 8%(w/v) polyacrylamide gel. After the gel was dried, autoradiography was carried out at −80 °C without using intensifying screen. Bands in the digests were assigned by comparison with Maxam−Gilbert markers specific for adenine and guanine.[28] The densitometric analysis was carried out using BIO-1D software from M&S Instruments Trading Inc. The footprintings were performed at least three times.

Acknowledgment. This research is supported by a Grand-in-Aid for Scientific Research on Priority Areas “Biometallics” (No. 08249103) for E.K.

JA983884J

(28) Maxam, A. M.; Gilbert, W. *Proc. Natl. Acad. Sci. U.S.A.* **1977**, *74*, 560−564.